Vlasov-kinetic computer simulations of electrostatic waves in dusty plasmas: an overview of recent results

S. M. Hosseini Jenab*
Department of Physics, South Tehran Branch, Islamic Azad University, Tehran, Iran

I. Kourakis†
Center for Plasma Physics, Department of Physics and Astronomy, Queen's University Belfast, BT7 1NN Northern Ireland, UK
(Dated: May 22, 2014)

A series of numerical simulations based on a recurrence-free Vlasov kinetic model using kinetic phase point trajectories are presented. Electron-ion plasmas and three-component (electron-ion-dust) dusty or complex plasmas are considered, via independent simulations. Considering all plasma components modeled through a kinetic approach, the linear and nonlinear behavior of ion acoustic excitations is investigated. Maxwellian and Kappa-type (superthermal) distribution functions are assumed, as initial conditions, in separate simulations for the sake of comparison. The focus is on the parametric dependence of ion acoustic waves on the electron-to-ion temperature ratio and on the dust concentration.

I. INTRODUCTION

Considering the textbook description of electrostatic waves in ordinary two-component (i.e., electron-ion) plasma, two typical modes occur as a standard rule. Firstly, Langmuir waves, i.e. oscillations of an inertial electron fluid against a massive ("stationary") ion background with $kv_{Ti} \ll kv_{Te} \ll \omega$ (where v_{Ti} and v_{Te} indicate the thermal velocity of the ions and of electrons, respectively, while ω denotes the angular frequency of the wave). Secondly, ion-acoustic (IA) waves (IAWs), in which ions provide the inertia, while the electrons behave as a background charge, providing the necessary restoring force[1].

In many real plasma situations, e.g. in astrophysical and in laboratory plasmas, a third component occurs, namely in the form of massive charged dust particulates, whose presence affects the charge balance and may play a crucial rule in shaping the plasma dynamics[2–4]. The dust particles have been shown to alter and even introduce new modes of electrostatic waves. In the presence of the dust component in the background, dust particles modify the charge balance, and ionic oscillations give rise to the so-called dust-ion acoustic (DIA) mode[5], characterized by frequency in the range $kv_{Td} \ll kv_{Ti} \ll \omega \ll kv_{Te}$. At the relevant scale, the electrons can be considered inertialess, the dust particles are practically stationary, while the ion population provides the inertia and the electron pressure, exerted through the electric field, plays the role of the restoring force. Furthermore, electrostatic oscillations of the dust component in the plasma give rise to a completely new branch of electrostatic waves, called dust-acoustic (DA) waves, with frequency lying in the range $kv_{Td} \ll \omega \ll kv_{Ti} \ll kv_{Te}$, implying such a low phase speed that an observer may actually track the wave with their own eyes[2].

Electrostatic plasma waves are subject to the well-known Landau-type damping mechanism[6], first predicted by L.D. Landau in 1946 for Langmuir waves[7]. This phenomenon basically describes a process of dissipation of macro-scale electric energy into micro-scale kinetic energy of particles, in fact even occurring in collisionless plasma. Linear and nonlinear Landau damping processes have been intensively studied in the past, theoretically, computationally and experimentally, and have been a standard focus in plasma research for decades. It is believed that *'approximately every third paper on plasma physics and its applications contains a direct reference to Landau damping'*[6]. Despite the wide literature in the topic, including investigations from both mathematical and physical viewpoints, there are still many challenging questions, especially in the nonlinear regime. A detailed mathematical theory for Landau damping has been presented recently by C. Villani[8]. Villani won the Fields medal, the most prestigious award in mathematics for this achievement, a fact which reflects the complexity and importance of the topic.

The *nonlinear* evolutions stage of Landau damping in plasmas has been shown to result in the formation of oscillatory BGK modes[9]. These are collective modes, first predicted by Bernstein, Greene and Kruskal[10] in collisionless, unmagnetized one-dimensional plasma, representing exact solutions of the Vlasov-Poisson set of equations, which are nonlinear, stationary and experience no damping. In the case of Langmuir waves, the existence of an initial field threshold has been shown, which separates the linear and nonlinear regimes[11–13]. Below this threshold, exponential decay of the waves occurs, while above the threshold, linear Landau damping turns out to be a transient phase which leads to non-zero time-asymptotic solutions in the form of BGK modes.

Due to its purely kinetic origin, the Landau damp-

*Email: mehdi.jenab@yahoo.com
†Email: IoannisKourakisSci@gmail.com; i.kourakis@qub.ac.uk

ing mechanism is treated by resorting to kinetic theory, i.e. in the case of collisionless plasma by directly solving the Vlasov equation[14]. The fundamental Vlasov kinetic equation has paved the way to the so-called kinetic simulation of plasmas. Various kinetic simulation approaches, involving different computational techniques to solve the Vlasov equation in combination with Maxwell equations, have been presented in the past. We note, among others, the splitting method[15], among the earliest attempts in this field, the Fourier transformation approach[16], the conservative scheme[17], and the semi-Lagrangian method, based on following phase-point trajectories[18]. All of these schemes in kinetic simulation are restricted by an inherent *recurrence effect*, namely the initial condition of the simulation reappears periodically at

$$\tau_r = \frac{2n\pi}{kdv} \qquad (n = 1, 2, 3, ...)\,, \tag{1}$$

where k and dv are the wavenumber and the grid step in the velocity direction respectively[15–20], hence the simulation results are valid only for $t < \tau_{r(n=1)}$. It is noted that the recurrence effect is purely artificial (numerical) and reflects no physical truth known so far. **It is worth mentioning that some of the simulation methods mentioned above have tried to solve this problem by adopting different techniques, mostly by increasing dv and avoiding the recurrence effect[17,20]; interestingly, open boundary conditions have been employed in the Fourier transformation approach[16], which appears to remove or at least suppress the recurrence effect.** Landau damping is a kinetic effect, so it essentially depends on the distribution function (statistics) of the plasma (precisely speaking, the shape of distribution function around the phase velocity). Of interest here is the occurrence of non-Maxwellian plasmas, bearing an excess in superthermal particle populations. Such "superthermal" plasmas were first studied in Space plasmas[21–23], where an *ad hoc kappa*-parametrized distribution function (df) was proposed[24] to explain the long tail appearing in the velocity distribution at high (velocity) values. This approach was subsequently proven to be very successful in modeling non-Maxwellian situations in various astrophysical and experimental plasma situations[25–30]. The kappa distribution function draws its name from a real parameter (κ), which measures the strength of the superthermal tail in the distribution function, reflecting the excess in highly energetic particles. For large κ the superthermal tail shrinks, and the Maxwellian distribution is recovered for $\kappa \to \infty$. The deviation from the Maxwellian df in superthermal plasmas ultimately modifies the features of electrostatic waves propagating in it, e.g., dispersion properties, solitary wave characteristics[31] and Landau damping rate[32,33].

Our aim in this article is to present some recent results, and also summarize earlier ones, here corroborated by more rigorous simulations. We focus on electrostatic waves in multicomponent plasmas, investigating their propagation characteristics and the occurrence of Landau damping, by adopting a unique methodology, i.e. by treating all plasma components via a Vlasov equation. In the simulation presented here, we have relaxed the mass ratio to its natural value of $M_i/M_e = 1836$, thus extending earlier results where a fictitious ratio of 100 was adopted[34], as a standard way to cope with computational constraints. We shall point out the parametric dependence of the dynamics on intrinsic plasma parameters, namely on the dust concentration, the temperature of each plasma constituent and, importantly, on the shape of distribution function. kappa-type and Maxwellian distribution functions are employed in separate simulations, to be critically compared in this report. By adopting a fully kinetic simulation approach, insight is gained in the plasma dynamics in a more rigorous way, in comparison to fluid model; furthermore, the kinetic method is free from statistical noise, e.g. ubiquitous in particle-in-cell (PIC) simulations[35–37].

The numerical procedure employed here is based on an original kinetic simulation algorithm, following phase point trajectories. Basic information needed in the following is briefly summarized here; interested readers are referred to, e.g., Ref. 18 for details. A Vlasov-type kinetic equation is considered for each of the plasma constituents. By applying a characteristics method, each of these equations is reduced to two first order differential equations which in turn are solved by using a leapfrog algorithm. Generally speaking, the phase points followed dynamically represent an ensemble of real particles with almost equal speed and coordinates in the spatial axes. Each phase point incorporates three quantities: the instantaneous value of the distribution function f associated with it, basically reflecting the number of particles it represents; the average speed v of real particles; and the average coordinates r of real particles, in the spatial axes. Throughout the temporal evolution of the simulation, r and v will vary, obeying the reduced two first-order differential equations, i.e., the Vlasov equation, while f remains fixed. By changing speed v and spatial coordinate r, the phase points move through the grid-cells –and grid-points– which are used to discretize the phase space, and this displacement results in a change in shape of the distribution function f, and thus the temporal evolution of the distribution function is observed and followed. The path of phase points in phase space is identical to the trajectories of real particles in the phase space, thus as Liouville's theorem dictates, the distribution function should remain constant on these trajectories, hence f remains fixed. In other known kinetic simulation techniques, the value of f is reconstructed repeatedly at each time step on the grid-points and numerical errors arise and accumulate inevitably, ultimately leading to a deviation from Liouville's theorem. By allowing for phase points "float-

ing" in phase space without being constantly constrained to grid-points, this method prevent the aforementioned anomalous recurrence effect from emerging through the numerical simulation. Detailed analysis shows that recurrence effect can be eliminated via a randomized allocation of phase points in the velocity direction at the initial stage of the simulation[38].

The layout of this paper goes as follows. In the following Section II, we introduce the basic aspects of our theoretical model. In Sections III and IV, two series of simulations of DIA waves in the linear regime, adopting a plasma in thermal equilibrium and a superthermal plasma, respectively, are presented and discussed. The nonlinear regime, i.e. BGK modes, is considered in Section V for two separate cases (Maxwellian and kappa-distributed electrons and ions). Section VI is associated to study of linear regime of dust-acoustic waves. The concluding Section VII is dedicated to a summary of our results.

II. MODEL AND NUMERICAL PROCEDURE

We will investigate the dynamical evolution of the plasma in the electrostatic approximation, based on the Vlasov-Poisson set of equations. We consider a a three-component plasma, namely comprising three elements: electrons (mass m_e, charge $q_e = -e$), singly ionized ions (mass m_i, charge $q_i = +e$) and negatively charged dust particles (mass m_d, charge $q_d = -Z_d e$). The dust charge (-Z_d) is assumed constant throughout, thus neglecting charge fluctuations and charging processes in our simulations. Our study relies on a (1+1)-dimensional approach, taking into account one dimension in space and one dimension in the velocity axis. Each of the (three) plasma constituents is modeled by its own Vlasov equation, viz.

$$\frac{\partial f_s(x,v,t)}{\partial t} + v\frac{\partial f_s(x,v,t)}{\partial x} + \frac{q_s E(x,t)}{m_s}\frac{\partial f_s(x,v,t)}{\partial v} = 0\,. \quad (2)$$

The subscript $s = e, i, d$ henceforth refers to the electron, ion or dust component, respectively, everywhere.

The electric field generation is modeled through Poisson equation:

$$\frac{\partial^2 \phi(x,t)}{\partial x^2} = -\frac{1}{\epsilon_0}\sum_{s=e,i,d}\rho_s\,. \quad (3)$$

The above equations are coupled via the density variable(s) appearing in the latter (Poisson) equation, which result from an integration of the distribution function as

$$\rho_s(x,t) = q_s n_s(x,t), \quad (4)$$

$$n_s(x,t) = n_{s0} N_s(x,t), \quad (5)$$

and

$$N_s(x,t) = \int f_s(x,v,t)dv\,. \quad (6)$$

Here, ρ, n_s and N_s represent the charge density, the scaled physical density and the (particle) number density, respectively, of each plasma species, while n_{s0} denotes the density at equilibrium.

At equilibrium, all three plasma elements are unperturbed, hence $N_{s0} = 1$, therefore the self-consistent electric field vanishes, since Poisson's equation then reads

$$\sum q_s n_{s0}(x,t) = 0\,. \quad (7)$$

Charge neutrality is thus assumed at equilibrium (only); this is often referred to as the *quasi-neutrality* hypothesis.

For computational convenience, the above set of equations (2)-(3) have been normalized, leading to dimensionless expressions, as outlined in the following. Space and time are scaled by λ_{Di} and ω_{pi}^{-1} respectively, where $\omega_{pi} = \sqrt{n_{i0}e^2/(m_i\epsilon_0)}$ is the ion plasma frequency and $\lambda_{Di} = \sqrt{\epsilon_0 K_B T_i/(n_{i0}e^2)}$ is the ion Debye length. Given our dynamical scale of interest, the velocity variable v has been scaled by the ion thermal speed $v_{th_i} = \sqrt{K_B T_i/m_i}$, while the electric field and the electric potential have been scaled by $K_B T_i/(e\lambda_{Di})$ and $K_B T_i/e$, respectively (here K_B is Boltzmann's constant). The densities of the three species are normalized by n_{i0}.

The dimensionless (reduced) Vlasov-Poisson set of equations read(s)

$$\frac{\partial f_s(x,v,t)}{\partial t} + v\frac{\partial f_s(x,v,t)}{\partial x} + q_s\frac{m_i}{m_s}E(x,t)\frac{\partial f_s(x,v,t)}{\partial v} = 0\,, \qquad (s = e,i,d) \quad (8)$$

where charges are normalized by $+e$ (viz., $q_e = -1$, $q_i = +1$ and $q_d = -Z_d$), and

$$\frac{\partial^2 \phi(x,t)}{\partial x^2} = \sum_{s=e,i,d}\rho_{s0}N_s(x,t), \quad (9)$$

where $\rho_{e0} = \sigma = n_{e0}/n_{i0}$, $\rho_{i0} = -1$ and $\rho_{d0} = \delta = Z_d n_{d0}/n_{i0}$. The normalized number density equation reads:

$$N_s(x,t) = \int f_s(x,v,t)\,dv. \quad (10)$$

Note that the parameters δ and σ are coupled through the quasi-neutrality condition:

$$\sigma = 1 - \delta\,. \quad (11)$$

The real parameter δ represents the (normalized) charge density of the dust particles and is fed to the simulations as a constant at the initial step: it serves

to regulate the role of the dust concentration. An ordinary electron-ion (dust-free) plasma is recovered, by setting δ to zero.

The simulation cycle for each time step starts by calculating the number density (N_s) of each species by integrating of distribution function over the velocities, via Eq.6, and then solving Poisson's equation (9) to obtain the self-consistent electric field. The latter (field) is then fed into the Vlasov equations (8) (for $s = e, i, d$) and the distribution functions for the next step is computed. This cycle is iterated in a step-by-step manner. The energy and entropy deviations (from their respective initial values) -which would indicate violation of conservation laws - are checked throughout each simulation, and were indeed verified never to exceed a reliability threshold (say, ≈ 0.001) throughout all the simulations presented herein.

The initial distribution function is determined for each of the elements at the initial step. In this study, we consider (separately) two types of distribution functions. First of all, we employ the well-known Maxwellian distribution function, modeling thermal equilibrium, in its normalized form:

$$f_s(x,0) = \sqrt{\xi_s \frac{1}{2\pi}} exp\big(-\xi_s \frac{v^2}{2}\big) \qquad (12)$$

where

$$\xi_s = \frac{m_s}{m_i}\frac{T_i}{T_s}\,, \qquad (s = e, i, d). \qquad (13)$$

Then, a *kappa*-type (κ) distribution function is adopted, in its normalized form[39]:

$$f_s(x,0) = \sqrt{\frac{1}{2\pi}\frac{\xi_s}{(\kappa-3/2)}}\frac{\Gamma(\kappa)}{\Gamma(\kappa-1/2)} \left[1 + \frac{\xi_s}{(\kappa-3/2)}\frac{v^2}{2}\right]^{-\kappa}. \qquad (14)$$

In order to trigger electrostatic excitations of the ionic component (DIA, dust-ion-acoustic mode) or of its dust counterpart (DA, dust-acouctic mode), the respective inertial element will be perturbed by imposing a monochromatic perturbation on the initial distribution function of that element, in the form: $f[1 + \alpha \cos\big(\frac{2\pi}{\lambda}x\big)]$, where α represents the strength of the perturbation and λ represents the wavelength (scaled by λ_{Di}). While small values of α are sufficient to excite linear waves, larger values will also be considered for the nonlinear stage to be triggered. The above perturbation is imposed either on the ion-distribution function or on the dust distribution function, in order to trigger DIA waves or DA waves, respectively.

The parameter values adopted in our simulations here are: $m_d/m_i = 10^5$, $m_i/m_e = 1836$, $T_i/T_d = 400$, $Z_d = 1000$, and time step $dt = 0.01$. Other parameters, like δ, $L = \lambda$ (=the length of the simulation box), α and T_e/T_i (hereafter θ) may vary in different sets of simulations, thus the respective values will be mentioned where appropriate. The grid applied for phase space discretization (M_x points in x-direction and M_{vx} points in the x-component of the velocity) is set to $(M_x, M_{vx}) = (25, 3000)$ for the linear regime. As a consequence, the phase space is covered by 7.5×10^4 cubic cells, and in each of the cells, at the initial step 4 phase points are scattered randomly - in order to avoid the aforementioned recurrence effect. Accordingly, the distribution function of each of the plasma elements is approximated by an array of 3×10^5 phase points. **Since we are using periodic boundary conditions in the x-direction, the number of phase points remains constant throughout the simulations.** In the nonlinear regime (i.e. to study BGK modes), longer time runs are needed, thus a finer grid with more cells is employed, to reduce the computational error in the later stages of the simulation.

III. ION-ACOUSTIC AND DUST-ION-ACOUSTIC VERSUS ELECTRON PLASMA (LANGMUIR) WAVES

a. Electron-ion (dust-free) plasma. We shall first investigate ion-acoustic waves. In order to enhance Landau damping, we focus on the region near (electron-to-ion temperature ratio) $\theta = 1.0$. For a start, we have consider electron-ion plasma (setting $\delta = 0$). The results are presented in Fig. 1; as expected, ion-acoustic waves are heavily damped, and cannot propagate in the plasma; therefore, no oscillation is observed in the (ion) number density.

For the sake of comparison, Langmuir waves have also been excited in separate simulation, by adopting the appropriate wavelength in the initial condition (all other parameter values being kept identical). A comparison of the two cases (both shown in Fig. 1) reveals that, while IA waves are severely damped, fading out after just one oscillation (note the ion number density in 1(b)), for the same plasma parameters, Langmuir waves do propagate, manifesting a clear exponential decay later due to Landau damping (note the electron number density 1(b)). For Langmuir waves, the perturbation is imposed on electrons and only Langmuir waves are excited (1(b)), while for IAWs, it is applied on the ions, where both Langmuir waves and IAWs are ignited (1(c)).

b. Dust-ion acoustic waves in dusty plasma. In the next step, the effect of the dust (setting $\delta \neq 0$) on the ion-acoustic wave characteristics are considered. The outcome of the simulation is shown in Fig.2b. As theoretically expected, by introducing dust particles, ion-acoustic waves do propagate in the plasma even for $\theta = 1.0$. Physically speaking, this striking fact is due to a dramatic modification of the phase velocity, due to the dust species, which removes resonant particles away from the wave reference frame. On the

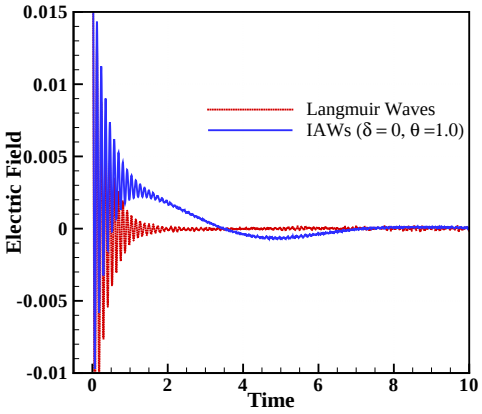

(a)

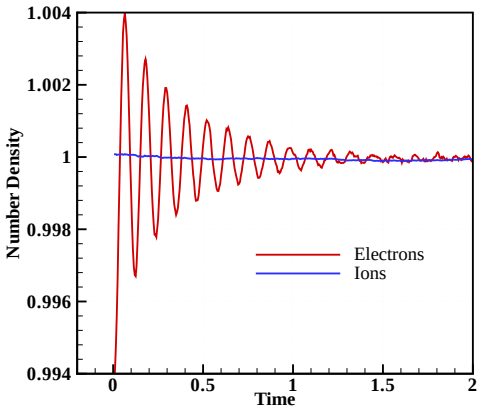

(b)

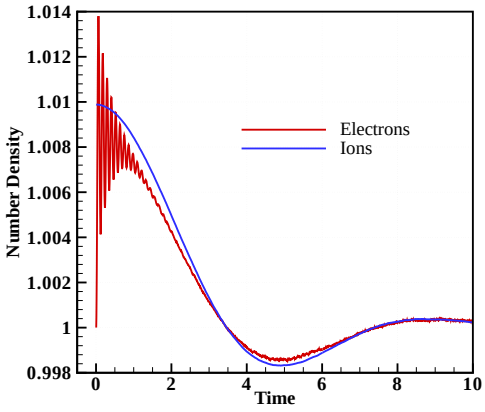

(c)

FIG. 1: (a) The evolution of the normalized electric field versus normalized time ($t\omega_{pi}$) is depicted, for *Langmuir waves* (red-dotted curve) and for *ion-acoustic waves* (blue-solid curve), for electron-ion plasma ($\delta = 0$), choosing $\theta = 1$). The normalized wavelength ($\lambda/\lambda_{Di} = 5\pi$) is kept the same in both cases shown. (b) The normalized number density of electrons (red-dotted curve) and ions (blue-solid curve) is depicted, for *Langmuir waves*. (c) The normalized number density of electrons (red-dotted curve) and ions (blue-solid curve) is shown versus normalized time (as above), for *ion-acoustic waves* (taking $\delta = 0$, $\theta = 1$, as in the other panels).

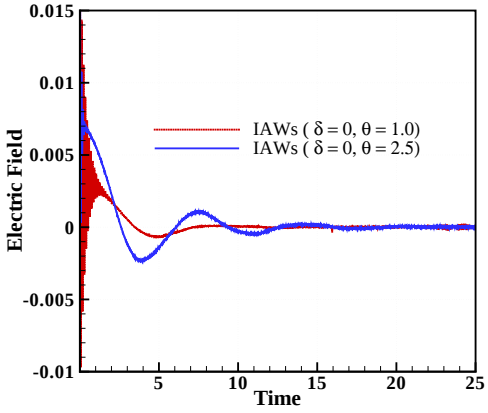

(a)

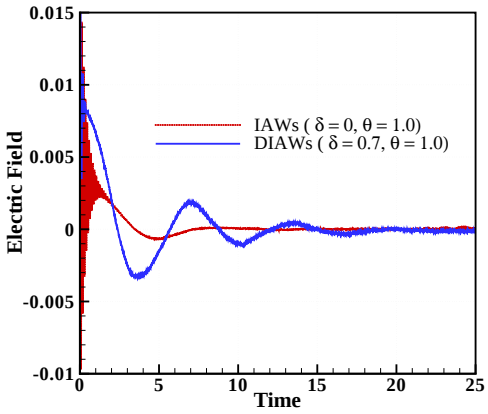

(b)

FIG. 2: The evolution of the (normalized) electric field versus (normalized) time is depicted, for three different combinations of δ and θ, in the case of ion-acoustic waves. (a) Comparison between [$\delta = 0$ & $\theta = 1$] (red-dotted cure) and [$\delta = 0$ & $\theta = 2.5$] (blue-solid curve): note that, by increasing the electron-ion temperature ratio, the Landau damping rate decreases and IA wave propagation becomes possible. (b) Comparison between [$\delta = 0$ & $\theta = 1$] (red-dotted cure) and [$\delta = 0.7$ & $\theta = 1$ (dust-ion-acoustic waves)] (blue-solid curve): having introduced the dust particles in the plasma, the Landau damping rate decreases.

other hand, Fig. 2a presents a similar observation of propagating ion-acoustic-waves, this time for higher θ.

Inspired by the qualitative results presented in Figs. 1 and 2, we are now ready to study the quantitative effect of (the electron-to-ion temperature ratio) θ and of (the dust parameter) δ on dust-ion-acoustic wavepackets. Here the focus is on the parametric dependence (variation) of the wave frequency and of the associated Landau damping rate on the above factors.

Summarizing the results shown in Fig. 3, the effect of increasing the **electron-to-ion temperature**

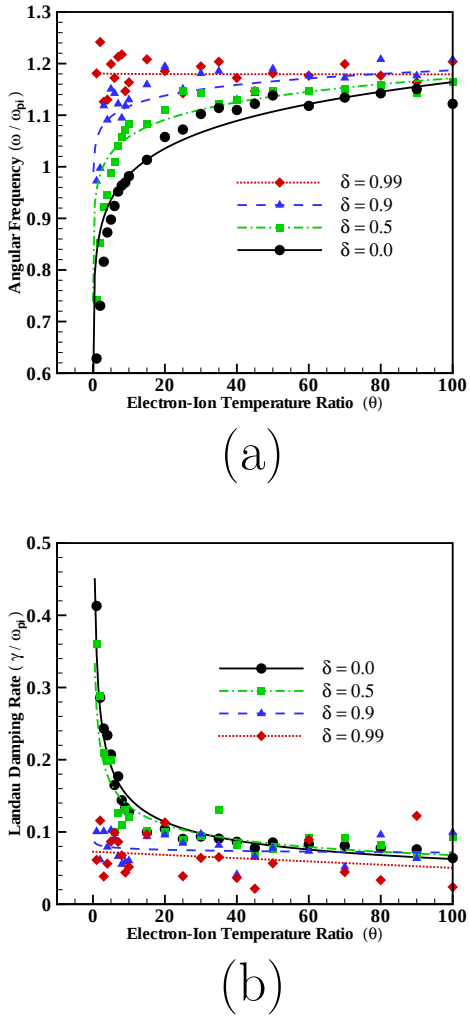

FIG. 3: (a) The effect of the electron-ion temperature ratio $\theta = T_e/T_i$ on the (scaled) frequency (ω/ω_{pi}) of IA and DIA waves is depicted for different values of $\delta = Z_d n_{d0}/n_{i0}$ (the normalized charge density of dust particles), taking $\lambda/\lambda_{Di} = 5\pi$, $dt = 0.01$, $\alpha = 0.01$ and 3×10^5 phase points. (b) The normalized Landau damping rate (γ/ω_{pi}) is depicted, for the same wave and for the same parameters as in the previous panel. As θ increases, the frequency also increases (practically exponentially), while the Landau damping rate drops, in what resembles qualitatively an exponential decay. However, this fact mostly applies to the cases of small δ, i.e. for weak dust concentration. Near the extreme case of full electron depletion ($\delta = 0.9$ or even as high as 0.99), both characteristics are independent from the electron-ion temperature ratio; this was somehow expected, since the role of electrons is rather limited under those circumstances.

ratio (θ) is significant upto a certain limit ($\theta \leq 30$), whereafter the picture remains practically unchanged for higher values. In the latter case, both factors tend to fluctuate around a saturation level which equals 1.15 and 0.08 for the frequency and for the linear Landau damping rate, respectively (both normalized by the ion plasma frequency). However, these dependencies are also sensitive to δ, in that as δ increases, the saturation level is attained for lower θ and, in fact, in the extreme case of $\delta = 0.99$ (quasi-complete electron depletion), the sharp and sensitive part no longer exists and only fluctuations around the saturation values are visible. **In this case, essentially we recover a two-species plasma consisting of immobile dust particles and ions vibrating against the stationary dust particle environment. Naturally, we recover waves with qualitative characteristics similar to Langmuir waves, since this situation mimics electron plasma oscillations in an electron-ion plasma, wherein electrons oscillate against a quasi-stationary massive ion background.** The fast drop in the Landau damping rate can be interpreted by considering that any increase in frequency (which entails a sharp increase for $\theta < 30$) results in modification of the phase velocity value, which in turns leads to a decrease in the first derivative of the distribution function around the phase velocity (affecting the distribution curve); this implies a drop in Landau damping rate, since the latter is directly related to the first derivative of the distribution function in the vicinity of the phase velocity. By exceeding $\theta \geq 30$, roughly, the electron distribution function around the DIA phase velocity is flattened enough for its first derivative to vanish, practically, thus electrons cannot behave as resonant particles, for Landau damping to occur. On the other hand, for higher values of θ, the ions alone cause Landau damping. Therefore, the (linear) Landau damping mechanism is no more sensitive to the electron properties, such as their temperature.

The dependence of DIA characteristics on the parameter δ follows a practically linear trend, as portrayed in Fig. 4: both quantities depicted follow a similar trend, thus the curves obtained for three different values of θ tend to 1.15 and 0.08, respectively, as $\delta \to 1.0$ for the (normalized) angular frequency and for the (normalized) linear Landau damping rate respectively. These two values follow from the asymptotic values in Fig. 3: this fact suggests that, either increasing the electron thermal velocity (via θ), or reducing the electron contribution by increasing δ (recall that $\delta = 1$ denotes full electron depletion in the plasma), results in a similar modification in the DIA wave properties.

An exhaustive discussion about the above analytical considerations and a comparison with theoretical results can be found in Ref. 34. We note that the ion-to-electron mass ratio was set to a fictitious value of 100 in Ref. 34, while it was relaxed to its natural value of 1836 in our simulations for this paper, the trend remains unchanged; furthermore, the values of the frequency and of the linear Landau damping rate in the depleted-electron case are practically identical, while the new simulations (based on the natural values of the mass-ratio) are in better agreement with

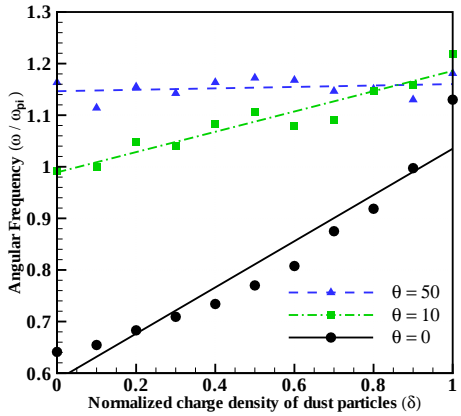

(a)

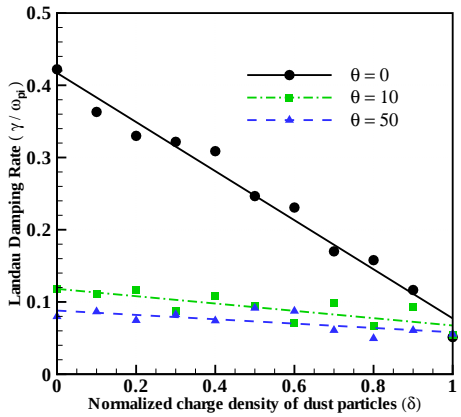

(b)

FIG. 4: (a) The normalized angular frequency (ω/ω_{pi}) of dust-ion-acoustic waves is depicted versus the (normalized) charge density of dust particles ($\delta = Z_d n_{d0}/n_{i0}$) for three different values of the electron-to-ion temperature ratio θ. (b) The (reduced) Landau damping rate (γ/ω_{pi}) is depicted in the same range as in the first panel. Both characteristics show a practically linear variation in δ. As δ grows, enhancement in frequency occurs while the Landau damping rate drops in value. However, the slope of either growth or fall decreases as θ increases.

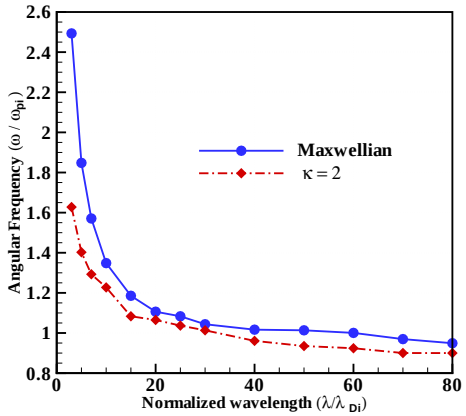

(a)

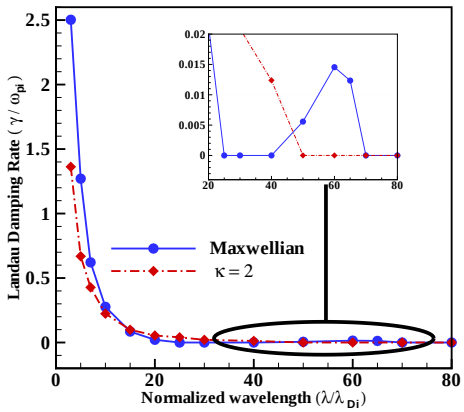

(b)

FIG. 5: (a) The (normalized) frequency (ω/ω_{pi}) is shown versus a large domain of normalized wavelength values (λ/λ_{Di}) (b) Fitting of the Landau damping rate (γ/ω_{pi}) of dust-ion-acoustic waves over the wavelength (λ/λ_{pi}) is shown, for two distinct distribution functions. Here, we have taken $\delta = 0.99$ and $\theta = 10$.

the theoretical values.

IV. THE EFFECT OF SUPERTHERMAL PARTICLES ON DUST-ION-ACOUSTIC WAVES

In order to study the effect of energetic (superthermal) ions and/or electrons on dust-ion-acoustic wave propagation, we adopt the kappa distribution function[31,39], adopting the same value of κ for both electrons and ions, for simplicity. Fig. 5 presents the outcome of a series of simulations for two extremely different distribution functions, namely considering a strongly non-Maxwellian distribution function with $\kappa = 2$ and the Maxwellian distribution function. As above, we have focused on the normalized frequency (ω/ω_{pi}) and the normalized Landau damping rate γ/ω_{pi}. These features are depicted against a wide range of normalized wavelength values (λ/λ_{Di}). As the wavelength grows, a sharp decrease is observed in both of these features and they both go down until they reach an asymptotic values, approximately zero for the Landau damping rate and almost 0.9 for the frequency. However, the details of this curve decline appear to differ between the two cases (distribution functions) considered. The *kappa* distribution function manifests a slower decline in Landau damping rate and acquires smaller value for the frequency.

It has been suggested by Villani[8] – and also by Landau in his original paper[7] – that linear Landau damping of Langmuir waves can only exist for small wavelengths in two-component plasmas. In this study, it was numerically shown that the same fact holds for DIA waves, although a three-component plasma model was consider in our study (and, generally speaking, Landau damping does not occur beyond a certain wavelength, say Λ). Note that the threshold Λ was found to differ between the two distribution functions considered herein: $\Lambda = \lambda/\lambda_{Di} \simeq 25$ for the Maxwellian distribution function, while $\Lambda = \lambda/\lambda_{Di} \simeq 50$ for the *kappa*-distribution function (with $\kappa = 2$, in the case considered). As shown in Fig. 5b, Landau damping may occur in a relatively narrow range of wavelength values, and the Landau damping rate in this domain actually presents a peak. The occurrence of the peak appears to be in qualitative agreement with Ref. 40. **Qualitatively speaking, one would expect that the peak is related to a change in phase speed[7]. Interestingly, the peak also appears, for certain parameter values, in a kinetic-theoretical study now in progress[43], and the qualitative explanation will be discussed therein. We plan to comment on this in separate future work[44].** Note that, due to computational noise, the weaker peak of the kappa distribution function cannot be tracked (in contrast with Ref. 42, where the noise was eliminated by using a much smaller ion-electron mass ratio).

V. BGK MODES ASSOCIATED WITH LARGE AMPLITUDE DUST-ION-ACOUSTIC WAVES

In order to push the ionic excitations into the nonlinear regime, the magnitude of the initial perturbation (α) imposed on the ions must be increased above a certain threshold. The existence of a threshold, above which Landau damping switches its long-time asymptotic behavior from zero to non-zero for Langmuir waves, has been discussed intensively in Refs 11–13. Fig. 6 suggests thats a similar transition occurs in dust-ion-acoustic waves. For $\alpha = 0.01$, which lies beneath the presumed threshold, a plain exponential damping occurs and the amplitude goes down to zero. On the other hand, for $\alpha = 0.05$ (seemingly above the threshold), Landau damping is observed until $t \leq 80$, beyond which the field amplitude decay stops and the amplitude subsequently starts to increase: a distinctive feature of nonlinear Landau damping. We have not attempted to trace the exact value of this threshold (say, roughly speaking, between $\alpha = 0.01$ and $\alpha = 0.05$), leaving this tedious task for future work. Nonlinear Landau damping results into the creation of BGK modes, in our case to be referred to as dust-BGK modes (or DBGK, hereafter)[45]. In Fig. 6, DBGK modes can be observed as a fluctuation over

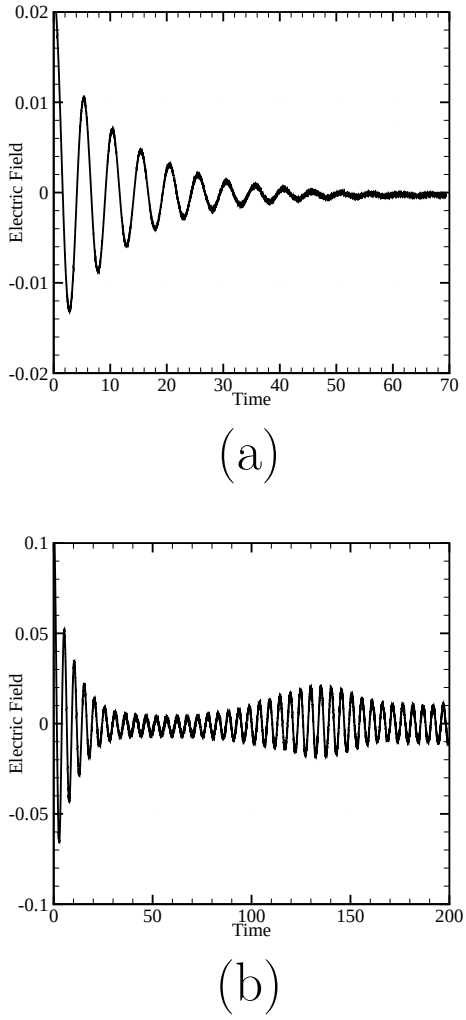

FIG. 6: (a) The evolution of the (normalized) electric field $E(e\lambda_{Di})/(K_B T_i)$ versus time (normalized by ω_{pi}) is depicted, for the case of $\lambda/\lambda_{Di} = 5\pi$, $\theta = T_e/T_i = 25$, $\delta = Z_d n_{d0}/n_{i0} = 0.5$ and $\alpha = 0.01$, in the range where linear Landau damping occurs. (b) The time evolution of the normalized electric field is depicted for the same parameters with $\alpha = 0.05$, which triggers nonlinear Landau damping and results to the occurrence of dust-BGK modes. The figure shows the first peak in thee dust-BGK amplitude, which appears around $t \approx 140\,\omega_{pi}^{-1}$.

the electric field amplitude, and are also associated with vortex formation in phase space, in the vicinity of the DIA phase velocity (c.f. Ref 46 for a detailed discussion).

In a generic manner, BGK modes are identified by two main characteristics, namely a characteristic time scale (*periodicity*) τ_{BGK} (here associated with the time interval between two successive peaks in the electric field amplitude) and by their *amplitude*, which is the value associated to the amplitude of the electric field at the peaks. These two characteristics are ultimately dependent on the phase space vortex re-

sponsible for the BGK modes. The temporal period of BGK modes originates from the vortex periodicity; as a matter of fact, upon considering the first rotation in phase space, this time is regarded as the *trapping time*. The amplitude, on the other hand, depends on the size of the vortex. Intuitively speaking, as the vortex grows in size, the amplitude increases along with it. In order to study the BGK mode profile here, we shall focus on the first peak of the field waveform, thus the first peak will be assumed to appear at time τ_{BGK}, and the field amplitude on the first peak will be taken as the amplitude of BGK modes.

Fig. 7, representing the dependence of the aforementioned quantities on the electron-ion temperature ratio θ, indicates the existence of a saturation level beyond $\theta \approx 30$, say, around 0.03 and 108 for the amplitude and the time scale, respectively. **The same trend was witnessed in Fig. 3 for linear Landau damping, and the saturation level for linear Landau damping rate also reaches around the similar value of $\theta \approx 30$. As a matter of fact, the linear and nonlinear Landau damping mechanisms are both strongly related to the shape of the distribution function for velocity values in the vicinity of the phase velocity, and also depend on the temperature (in turn affecting the shape of the distribution function); therefore they are arguably expected to have similar qualitative features.** Fig. 8 focuses on the effect of the dust particle concentration, i.e. via the normalized dust charge density parameter δ. The intrinsic characteristics of the DBGK excitations (periodicity and amplitude) depend on δ in a quasi-linear manner, while the slope of the curve decreases as θ increases. Again, the trend is reminiscent of Fig. 4 for linear Landau damping.

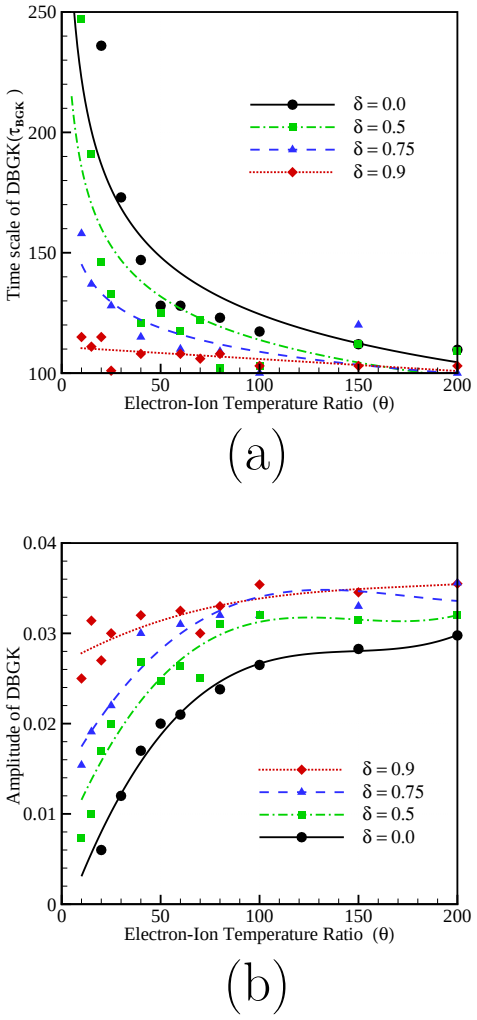

FIG. 7: (a) The characteristic time scale (periodicity) of DBGK modes, τ_{BGK}, is depicted versus the electron-to-ion temperature ratio θ, for three different values of δ. The remaining parameters are taken as: $\lambda/\lambda_{Di} = 5\pi$, $\alpha = 0.05$ **and 8×10^5 phase points are used for sampling**. As θ increases, τ_{BGK} decreases, until an asymptotic value, here about ≈ 108. The appearance time of the first peak is depicted in this plot. (b) The dependence of the DBGK wavepacket amplitude on the electron-to-ion temperature ratio θ is shown, for three different values of δ. The amplitude is seen to grow with θ, while its intensity drops. The asymptotic value attained for $\theta \geq 30$ can be seen to be around ≈ 0.03. The first electric field peak amplitude is considered in this plot.

VI. DUST-ACOUSTIC WAVES

For the sake of comparison and for later reference, we shall now briefly focus on dust-acoustic waves and, in particular, on the effect of Lorentzian plasma - modeled by kappa distribution function- on those.

In order to trigger low-frequency dust-acoustic waves, the perturbation is applied to the dust distribution function, which follows the Maxwellian distribution. The other two species, namely electrons and ions, follow a Maxwellian distribution function in one set of simulations and a kappa distribution functions in another.

The results of the two sets of simulations are presented in Fig. 9, showing acceptable qualitative agreement with earlier (analytical) results[47].

The simulations presented herewith are still at an early stage. A detailed investigation will be presented in forthcoming work.

VII. CONCLUSIONS

A recurrence-free, fully kinetic simulation approach has been adopted as a dynamical model for electrostatic waves in dusty plasma, focusing on the linear (weak amplitudes) and on the nonlinear (stronger amplitude) regime. In the former case, the plasma response was probed, in the form of the wave frequency and the instability (Landau damping) rate, tracing

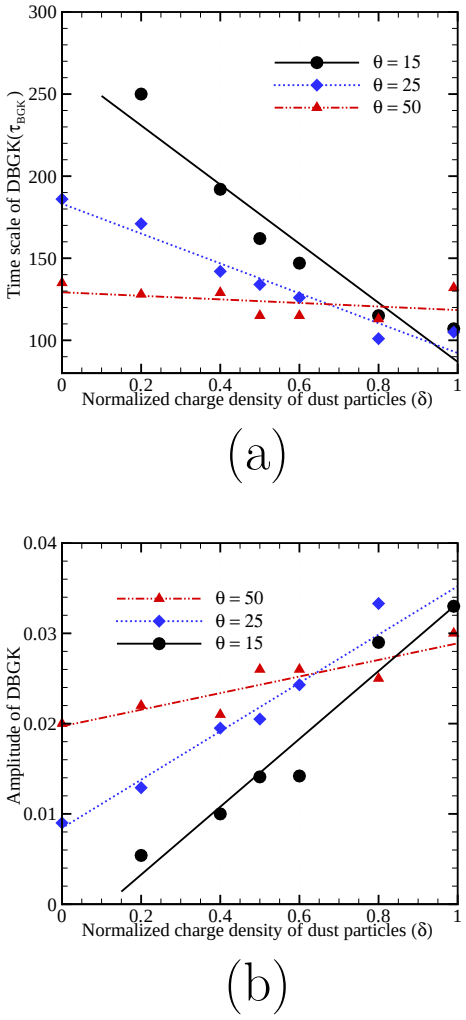

FIG. 8: (a) The relationship between the amplitude of DBGK modes (first peak, A_1) and the (normalized) dust charge density δ is shown, for three different values of θ. An increase in δ results in a practically linear increase in the amplitude. The three different curves obtained for different θ tend to the same value (0.035) for $\delta \to 1$. (b) The relationship of the trapping time τ_{BGK} of BGK modes on the (normalized) dust charge density δ is depicted, for different values of θ.

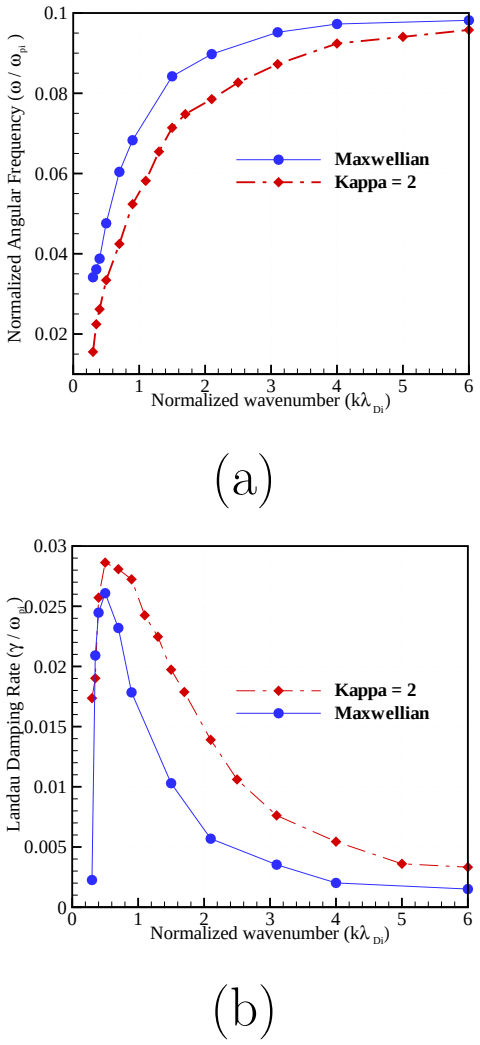

FIG. 9: (a) The Landau damping rate (γ) of dust-acoustic wavepackets –normalized by $1/\omega_{pi}$– is depicted versus the wavenumber k (normalized by the ion Debye length λ_{Di}) for two different distribution functions, in the range of $0 < k\lambda_i < 10$, namely $\kappa = 2$ (black, solid line) and Maxwellian ($\kappa \to \infty$)(blue, dotted line). A peak in γ appears around $0.5 < k\lambda_i < 2$ for both distribution functions. However the width and hight of these peaks varies for them. The results displays an acceptable agreement with analytical results[47] (b)Frequency of dust-acoustic waves versus wavenumber (k) –normalized by ion Debye length λ_i– is shown.

their dependence on the three main parameters of relevance: the electron-ion temperature ratio (θ), the dust charge density (δ) and the effect of non-thermality, expressed via different distribution functions.

We have shown that, by increasing the electron-ion temperature ratio θ above a certain threshold (which in turn depends on the value of δ), the effect of the electron dynamics on the propagation of electrostatic waves disappears. Good qualitative agreement was found with an earlier study[34], which relied on a small (fictitious) ion-to-electron mass ratio.

Two features of dust-BGK modes have been investigated parametrically, namely the periodicity τ_{BGK} and the amplitude; these were both shown to vary proportionally with the dust charge density δ, while they appeared to "saturate" to an asymptotic value when varied against θ. This qualitative result remained unchanged in the nonlinear regime.

We have also presented evidence that bigger phase space vortices arise by increasing the electron-to-ion temperature ratio θ, leading to stronger BGK modes. This can be justified by paying attention to the role of the electrons. As θ increases, hotter electrons can move more easily and leave the potential well associated with BGK modes. This in turn increases the

electric field amplitude, hence the amplitude of DBGK structures, and results in stronger BGK modes and thus bigger vortex in phase space. The net result is a substantial velocity difference between the two ends of the vortex (in velocity space). This means that the vortex spins faster, and the time periodicity of the BGK structures becomes shorter. It appears that the periodicity of dust-BGK modes decreases exponentially as the electron-ion temperature ratio (θ) increases.

As regards the dependence on the normalized dust charge density δ, a similar qualitative result holds (cf. Figs. 8 and 4), yet in this case presenting a practically linear curve trend. In the linear regime, the simulation results coincide quite accurately with the theoretical expectation. In the nonlinear regimes, on the other hand, our results provide inspiration for future theoretical investigations. Admittedly, the question of DBGK structure stability, lying beyond the scope of our study, remains unanswered, thus work on this direction is anticipated.

The effect of excess superthermal populations of ions or/and electrons was investigated in Figs.5 and 9, respectively, for DIA and for DA waves. It was shown that, as expected theoretically, a sharp decline occurs in the linear Landau damping rate as the wavelength is increased. A peak was observed in the Landau damping rate around some wavelength value in both cases considered, in qualitative agreement with earlier theoretical considerations[40,41,47]. Finally, it is worth mentioning, for the sake of rigor, that a few differences between theoretical and simulation results can be identified for DIA waves, in particular; these will be discussed in detail in forthcoming work[44] (discussion omitted here, for brevity).

Acknowledgments

Professor Manfred A. Hellberg (University of Kwazulu-Natal, Durban, South Africa) is warmly acknowledged for a number of inspiring discussions.

[1] F. F. Chen, *Introduction to Plasma Physics and Controlled Fusion: Plasma physics*, (Plenum Press, New York, 1984).
[2] Sergey V. Vladimirov, Kostya Ostrikov, Alex A. Samarian, *Physics and Applications of Complex Plasmas*, (Imperial College Press, 2005).
[3] D A Mendis, Plasma Sources Sci. Technol **11**, A219 (2002)
[4] P. K. Shukla, Phys. Plasmas **8**, 1791 (2001)
[5] P. K. Shukla, V. P. Silin, Phys. Scripta. **45**, 508 (1992)
[6] Ryutov, D. D. . Plasma Phys. Control. Fusion **41**, A1A12 (1999).
[7] Landau, L.D. *On the vibration of the electronic plasma.* J. Phys. USSR **10** 25 (1946). [English translation in JETP 16, 574. Reproduced in Collected papers of L.D. Landau, edited and with an introduction by D. ter Haar, Pergamon Press, 1965, pp. 445460; and in Men of Physics: L.D. Landau, Vol. 2, Pergamon Press, D. ter Haar, ed. (1965)].
[8] C. Mouhot, C. Villani, Acta Mathematica **207**, 1 (2011)
[9] T. M. ONeil, Phys. Fluids **8**, 2255 (1965)
[10] I. B. Bernstein, J. M. Greene, M. D. Kruskal, Phys. Rev **108**, 546 (1957)
[11] C. Lancellotti, J. J. Dorning, Phys. Rev. Lett **81**, 5137 (1998)
[12] C. Lancellotti, J. J. Dorning, Phys. Rev. E **68**, 026406 (2003)
[13] M. C. Firpo, Y. Elskens, Phys. Rev. Lett **84**, 3318 (2000)
[14] A. A. Vlasov, J. Exp. Theor. Phys **8**, 291 (1938) A. Vlasov, Soviet Phys. Uspekhi **10**, 721 (1968)
[15] C. Z. Cheng, G. Knorr, J. Comput. Phys **22**, 330 (1976)
[16] B. Eliasson, J. Comput. Phys **225**, 2 (2007)
[17] E. Sonnendrucker, P. Bertrand, J. Comput. Physics **22**, 1 (2001)
[18] F. Kazeminezhad, S. Kuhn, A. Tavakoli, Phys. Rev. E **67**, 026704 (2003)
[19] T. Minoshima, Y. Matsumoto, T. Amano, J. Comput. Phys **230**, 6800 (2011)
[20] G. Manfredi, Phys. Rev. Lett. **79**, 2815 (1997)
[21] V.M.Vasyliunas, J. Geophys. Res.**73**, 2389 (1968)
[22] B.Abraham-Shrauner, W.C.Feldman, J. Plasma. Phys **17**, 123 (1977)
[23] B.Abraham-Shrauner, J.R.Asbridge, S.J.Bame, W.C.Feldman, J. Geophys. Res **84**, 553 (1979)
[24] V. M. Vasyliunas, J. Geophys. Res **73**, 2839, (1968)
[25] M. A. Hellberg, R. L. Mace, R. J. Armstrong, G. Karlstad, J. Plasma. Phys **64**(4), 433 (2000)
[26] M. V. Goldman, D. L. Newman, A. Mangeney, Phys. Rev. Lett **99**, 145002 (2007)
[27] G. Sarri, M. E. Dieckmann, C. R. D. Brown, C. A. Cecchetti, D. J. Hoarty, S. F. James, R. Jung, I. Kourakis, H. Schamel, O. Willi, M. Borghesi, Phys. Plasmas **17**, 010701 (2010)
[28] V. Pierrard, M. Lazar, Solar Phys **267**, 153 (2010)
[29] G. Livadiotis, D. J. McComas, J. Geophys. Res **114**, 11105 (2009)
[30] G. Livadiotis, D. J. McComas, Astrophys. J. **714**, 971 (2010)
[31] I. Kourakis, S. Sultana, M.A. Hellberg, Plasma Phys. Control. Fusion. **54**, 124001 (2012)
[32] R. L. Mace, M. A. Hellberg, Phys. Plasmas **16**, 072113 (2009)
[33] T.K. Baluku, M.A. Hellberg, paper P5.176, in Proc. 39th EPS Conf. on Plasma Phys. & 16th Int. Congress on Plasma Phys. (2-6 July 2012, Stockholm, Sweden); available online at: http://ocs.ciemat.es/EPSICPP2012ABS/pdf/P5.176.pdf (accessed 24 Feb. 2014)
[34] S. M. Hosseini Jenab, I. Kourakis, H. Abbasi, Phys. Plasmas **18**, 073703 (2011)
[35] G. Sarri, M.E. Dieckmann, I. Kourakis, M. Borghesi,

Phys. Rev. Lett **107**, 025003 (2011)
[36] M.E. Dieckmann, A. Bret, G. Sarri, E. Perez Alvaro, I. Kourakis, M Borghesi, Plasma Phys. Cont. Fusion **54**, 085015 (2012)
[37] M.E. Dieckmann, G. Sarri, G.C. Murphy, A. Bret, L. Romagnani, I. Kourakis, M. Borghesi, A. Ynnerman, L.O.C. Drury, New J. Phys **14**, 023007/1-19 (2012)
[38] H. Abbasi , M. H. Jenab, H. Hakimi Pajouh, Phys. Rev. E **84**, 036702 (2011)
[39] M. A. Hellberg, R. L. Mace, T. K. Baluku, I. Kourakis, N. S. Saini, Phys. Plasmas **16**, 094701 (2009)
[40] Myoung-Jae Lee, Curr. Appl. Phys **10**, 1340 (2010)
[41] Myoung-Jae Lee, J. Korean Phys. Soc **46**, 5 (2005)
[42] S. M. Hosseini Jenab, T. Baluku, M.A. Hellberg, I. Kourakis, *Kinetic simulation approach to studying the Landau damping rate of dust-ion-acoustic waves in kappa-distributed plasmas*, Presented at the International Topical Conference in Plasma Science – ITCPS 2012, (Faro, Portugal).
[43] Manfred A. Hellberg (University of Kwazulu-Natal, Durban, South Africa), private communication.
[44] S. M. Hosseini Jenab, M.A. Hellberg, I. Kourakis, *Kinetic simulation of dust-ion-acoustic waves in kappa-distributed plasmas*, in preparation.
[45] M. Tribeche, R. Hamdi, T. H. Zerguini, Phys. Plasmas **7**, 4013 (2000)
[46] S. M. Hosseini Jenab, I. Kourakis, Phys. Plasmas **21**, 043701 (2014)
[47] Myoung-Jae Lee, Phys. Plasmas **14**, 032112 (2007)